Research Square

Preprints are preliminary reports that have not undergone peer review.
They should not be considered conclusive, used to inform clinical practice,
or referenced by the media as validated information.

Bioactivity-Guided Separation of Potential α-glycosidase Inhibitor from Clerodendranthus Spicatus based on HSCCC with Molecular Docking

Chunsheng Zhu
First Affiliated Hospital of Zhengzhou University
Hongjuan Niu
Minzu University of China
Anzheng Nie
First Affiliated Hospital of Zhengzhou University
Meng Bian (bianmeng0208@163.com)
First Affiliated Hospital of Zhengzhou University

Research Article

Keywords: Clerodendranthus Spicatus (Thunb), HSCCC, α-glycosidase inhibitor, molecular docking

Posted Date: December 28th, 2020

DOI: https://doi.org/10.21203/rs.3.rs-122251/v1

License: This work is licensed under a Creative Commons Attribution 4.0 International License.
Read Full License

Version of Record: A version of this preprint was published at Scientific Reports on March 25th, 2021. See the published version at https://doi.org/10.1038/s41598-021-86379-9.

Abstract

Clerodendranthus Spicatus is a traditional Dais medi-edible plant and it has been proven to have good blood glucose-lowering efficacy. However, the material basis of *Clerodendranthus Spicatus* has not been clarified yet. Therefore, in this paper, the compounds were purified by high-speed counter-current chromatography (HSCCC) and the potential activity of compounds were determined by molecular docking. In the separation process, the solvent system was determined by a 9 × 9 map-based solvent selection strategy and the solvent system hexane/ethyl acetate/methanol/water (3:5:3:5, v/v) was used for HSCCC. Finally, five compounds were purified and identified as 2-Caffeoyl-L-tartaric acid (1), N-(E)-caffeoyldopamine (2), rosmarinc acid (3), Methyl rosmarinate (4), 6,7,8,3',4'-Pentamethoxyflavone (5). Then, the identified compounds were individually docked with α-glycosidase. The affinity energies of the identified compounds ranged from -7.6 to -8.6 kcal/mol, which are all better than acarbose (-6.6 kcal/mol). In particularly, rosmarinc acid with the lowest affinity energy of -8.6 kcal/mol was wrapped by the active site of α-glycosidase. The docking results indicated that the target compounds have potential α-glycosidase inhibitory activity and may be responsible for the blood glucose-lowering activity of *Clerodendranthus Spicatus*. The results indicated that the bioactivity-guided method is practical for the effective separation of active compounds from natural resources.

1. Introduction

Diabetes is a serious chronic metabolic disorder affecting 463 million of individuals worldwide in 2019, and a further 700 million likely to be added by 2045[1]. Additionally, numerous epidemiological studies have shown that diabetes is not only closely related to blindness, limb amputations, and renal failure, but also an independent risk factor for peripheral artery disease[2–4]. Indeed, diabetes can be categorized into two types: T1D is mainly caused by insufficient insulin secretion, and T2D is abnormal insulin secretion and/or non-insulin-dependent diabetes, complicated by postprandial hyperglycemia[5,6]. Moreover, and remarkably, according to clinical statistics, only 5–10% of diabetics are affected by T1D, while T2D accounts for more than 90% of diabetes cases[7,8]. It is well known that the inhibition of carbohydrate-related enzymes like α-glycosidase by delaying glucose absorption, including acarbose, miglitol, and voglibose, is one of the effective controlling methods to overcome postprandial hyperglycemia [8]. However, long-term using these drugs exhibits a series of undesired side effects on the digestive system, such as abdominal pain, diarrhoea and nausea[9,10]. Accordingly, screening new α-glycosidase inhibitors to develop the new drugs with fewer side effects has been a research hotspot in recent years.

Clerodendranthus spicatus (Thunb.) C. Y. Wu (*C. spicatus*), popularly known as “Orthosiphon” or “kidney tea”, is a perennial herb of the Labiatae family, which is an endemic specie distributing in southern of China, such as Yunnan, Fujian and Guangxi provinces[11,12]. *C. spicatus* is a kind of medi-edible plant medicine, which has been used as an herbal remedy for gout, acute and chronic nephritis in Dai medicine with a history of more than 2,000 years in local ethnic groups in Yunnan Province, China[13,14]. In addition, earlier report had indicated that this plant contains high amount of flavonoids, phenolic acids,

anthraquinones and other ingredients[15]. Moreover, modern pharmacological studies have shown that the extracts of *C. spicatus* exhibit a significant effect on hypoglycemic effect, which can significantly lower the blood glucose levels in the streptozotocin-induced diabetes mouse model [16]. Therefore, there is a high possibility to screen and isolate the target components from *C. spicatus* as potential target therapeutic components for diabetes.

However, of note, the pharmacological activities were conducted on the complex extracts and it remained unclear which of the components in the crude extracts were active compounds and how each of these active components contributed to the pharmacological effects. As such, in order to well study the pharmacological activities, large amount of these compounds is needed, and an efficient method for separation of the compounds is a major task. As a no solid packing required chromatography, high-speed counter-current chromatography (HSCCC) is not limited by the solid stationary phase and has a larger sample load, and the use of solvent system avoids the use of solid chromatographic fillers and reduce the separation cost[17]. Meanwhile, the selection of thousands of different proportional solvent systems increases the possibility of successful separation of polar similar compounds by HSCCC[18,19]. Thus, HSCCC gradually became a crucial technique for separating the compounds from the natural products[20].

Nowadays, the studies of active compounds and efficacy-organ/tissue-cell-receptor/channel are faced with the adversity of high cost[21]. Fortunately, the interaction of the screening compounds and the potential targets can be predicted by molecular docking. Docking analyses were carried out for all molecules included in this study to predict the interaction between ligand and active site of receptor by energy-based scoring function[22]. Therefore, in the present study, the compounds were separated and purified by HSCCC, and then evaluate the interaction between α-glycosidase and the target compounds by molecular docking to predict whether the target compounds could be potential functions as α-glycosidase inhibitors, so as to provide reference for the development of new diabetes drugs.

2. Results And Discussion

2.1 Selection of solvent system

A successful separation of target compounds using HSCCC requires a careful search for a suitable two-phase solvent system that could provide an ideal range of partition coefficients (K). K values in the range of 0.2 to 5.0 are generally considered to be appropriate for HSCCC separation[20]. In addition, the separation factor between the two components ($\alpha = K1/K2$, $K1 > K2$) should be greater than 1.5[23]. Furthermore, the target compounds must be stable and soluble in such a solvent system, and the solvent system must separate clearly and quickly into two phases, and the solvent system must separate quickly into upper and lower phase in 30 seconds[20].

More recently, Liang et al. [24]successfully developed a new solvent selection strategy for targeted counter-current chromatography purification of natural products based on HEMWat 9 × 9 map. Particularly, it is

easier to get a suitable solvent system through making a simple screening 2□4 HEMWat two-phase solvent systems to obtain the sweet line or sweet zone without special knowledge, which is of great help to the separation of traditional Chinese medicine. Hence, in the present paper, an HEMWat 9 × 9 map-based solvent selection strategy was used. The key of the solvent selection strategy is to establish a linear regression equation using two solvent systems in the same line-group. Based on the diagonal lines of the HEMWat 9 × 9 map, HEMWat (1:5:1:5) (□) and HEMWat (5:5:5:5, v/v) (□) were chosen to find the linear regression equation of log *K* versus content of hexane number of solvent systems. According to the K value of the compounds, we find that the K value of compound 1 is minimum in the HEMWat. Thus, the compound 1 was selected as standard compound for linear regression. The K values of the standard compound were measured respectively with K□ at 0.71 and K□ at 2.04 respectively. Then, a linear regression equation “y = 0.1549x-0.4647” was obtained, where x is the hexane number of the solvent system and y is the log K. According to the regression equation, the appropriate system (K = 1) was determined as HEMWat (3:5:3:5, v/v). Further, the *K* value of the standard compound 1 in the solvent system was determined to be 1.13 which was very close to the predicted value. Thus, the solvent system was confirmed for further study.

Then, K values of the target compounds were then confirmed. As shown in Table 1, the α values between compounds 3 and 2 was lower than 1.2, which indicated that the two compounds cannot be achieved baseline separation in one step. Therefore, an appropriate polarity regulator was needed to alter the distribution of the target compounds. In the study, the acetic acid was used to change the distribution of the target compounds in the solvent system. Different volume ratios of acetic acid were added in solvent system HEMWat (3:5:3:5, v/v). As shown in Table 1, with the increasing of the acetic acid, the K value of compound 1 almost keep unchanged, while the K value of compounds 2, 3 and 4 were decreased clearly. In the solvent system HEMWat (3:5:3:5, v/v), K_4 was higher than K_2, with the acetic acid added in, the K_2 was higher than K_4, which indicated that the distribution of compounds 2 and 4 in the solvent system were reversed. As shown in Table 1, the K value of the target compounds were all in a proper range, but the α of compounds 2 and 4 in HEMWat (3:5:3:5, v/v) (0.5% acetic acid), and the α of compounds 2 and 3 in n-hexaneHEMWat (3:5:3:5, v/v)(1.0% acetic acid) both lower than 1.2, which indicated that these compounds are difficult to achieve baseline separation during the HSCCC. Fortunately, the target compounds had proper K values and α values in HEMWat (3:5:3:5, v/v) (1.5% acetic acid). Thus, acetic acid can be used as an effective solvent system polarity regulator and HEMWat (3:5:3:5, v/v) (1.5% acetic acid) was finally chosen to be the final choice for HSCCC process.

Table 1
The *K* values of the target compounds

Solvent System		K_1	K_2	K_3	K_4
HEMWat	3:5:3:5	1.13	4.94	2.64	5.23
HEMWat (0.5% acetic acid)	3:5:3:5	1.13	3.57	2.59	3.48
HEMWat (1.0% acetic acid)	3:5:3:5	1.09	2.33	2.41	2.11
HEMWat (1.5% acetic acid)	3:5:3:5	0.98	1.93	2.34	1.48

2.2 HSCCC process

The HSCCC process was carried out using HEMWat (3:5:3:5, v/v) (1.5% acetic acid) with other parameters: revolution speed, 800 rpm; flow rate, 2.0 mL/min; temperature, 30 ºC; 20 mg of the sample was dissolved in 10 mL of the lower phase with forth continuous sample injection in a single run (Fig. 2). There are four fractions collected and analyzed by HPLC (Fig. 3). Under the condition, 26 mg of compound 1, 42 mg of compound 3 + 5, 17 mg of compound 2, 23 mg of compound 4, were obtained from 160 mg sample. HPLC analysis showed that the purities of compounds 1, 2, 4 were higher than 98%. And the fraction of compounds 3 + 5 was further purified by preparative HPLC (prep-HPLC).

2.3 prep-HPLC purification

Because prep-HPLC has excellent column efficiency, high-throughput purification, and separation reproducibility, it is widely used in the separation of herbal medicines[25]. Hence, in the present study, prep-HPLC was used for further purification of these two compounds (compounds 3 + 5). From the condition of HPLC analysis of the sample, target compounds could be eluted when the concentration of methanol reached 40%. Thus, isocratic elution modes with 40% methanol were adopted in our experiment (Figure. 4). As a result, the target compounds were well separated, and 8 mg compound 3 and 40 mg compound 5 were obtained. HPLC analysis (Figure. 5) showed that the purities were higher than 98% after prep-HPLC purification.

2.4 Structural identification

The chemical structures of the five compounds were elucidated by ^{1}H-NMR and ^{13}C-NMR and were identified as 2-Caffeoyl-L-tartaric acid (1), N-(E)-caffeoyldopamine (2), rosmarinc acid (3), Methyl rosmarinate (4), 6,7,8,3',4'-Pentamethoxyflavone (5) (Figure. 6). Compounds 3 and 5 were separated from *C. spicatus* for the first time. The detailed data were as follows:

2-Caffeoyl-L-tartaric acid (1): 1H NMR (400 MHz, DMSO-d_6) δ 12.97 (1H, s, 5-OH), 10.42 (1H, s, 4'-OH),7.44 (2H, d, J = 8.1 Hz, H-2', 6'), 6.88 (2H, d, J = 8.1 Hz, H-5', 3'), 6.71 (1H, s, H-3), 6.70 (1H, d, J = 2.0 Hz, H-8), 6.42 (1H, d, J = 2.1 Hz, H-6), 5.04 (1H, s, H-1''). 13C NMR (100 MHz, DMSO-d_6): δ 182.58 (C-4), 164.37 (C-2), 163.01 (C-7), 161.46 (C-5), 161.13 (C-4'), 158.90 (C-9), 128.82 (C-2', 6'), 119.62 (C-1'), 116.38 (C-3',

5'), 113.61 (C-10), 102.49 (C-3), 99.67 (C-1"), 99.41 (C-6), 91.93 (C-8), 77.75 (C-5"), 77.02 (C-3"), 74.61 (C-2"), 70.38 (C-4"), 61.34 (C-6"). Compared with literature[26], it was identified as 2-Caffeoyl-L-tartaric acid.

N-(E)-caffeoyldopamine (2): ^{1}H NMR (400 MHz, DMSO-d_6) δ: 3.06–3.43 (6H, m, glc-1", 2", 3", 4", 5", 6"), 3.91 (3H, s, H-7-OMe), 5.04 (1H, d, J = 7.2 Hz, H-1"), 6.74 (1H, s, H-3), 6.88 (1H, s, H-8), 6.91 (1H, d, J = 8.2 Hz, H-3'), 7.46 (2H, m, H-2', 6'), 9.43 (1H, s, H-3'-OH), 10.01 (1H, s, H-4'-OH), 13.09 (1H, s, H-5-OH). ^{13}C NMR (100 MHz, DMSO-d_6) δ: 56.54 (C-OMe), 60.88 (C-6"), 69.75 (C-2"), 74.14 (C-4"), 76.55 (C-5"), 77.29 (C-3"), 91.52 (C-8), 101.99 (C-1"), 102.70 (C-3), 104.39 (C-10), 113.52 (C-2'), 115.94 (C-5'), 119.05 (C-6'), 121.47 (C-1'), 128.10 (C-6), 145.77 (C-3'), 149.80 (C-4'), 151.70 (C-9), 152.57 (C-5), 158.51 (C-7), 164.19 (C-2), 182.13 (C-4). Compared with literature[27], it was identified as Pedaliin.

rosmarinc acid (3): ^{1}H NMR (400 MHz, DMSO-d_6) δ: 7.56 (1H, d, J = 2.1 Hz, H-2'), 7.53 (1H, dd, J = 2.1, 8.1 Hz, H-6'), 6.84 (1H, d, J = 8.2 Hz, H-5'), 6.39 (1H, d, J = 1.9 Hz, H-8), 6.19 (1H, d, J = 1.9 Hz, H-6), 5.33 (1H, d, J = 7.2 Hz, H-1"), 4.39 (1H, s, H-1"), 3.71 (2H, d, J = 9.7 Hz, H-6"), 1.00 (3H, d, J = 6.1 Hz, CH_3-6'"). ^{13}C NMR (100 MHz, DMSO-d_6) δ: 177.78 (C-4), 164.67 (C-7), 161.65 (C-5), 157.02 (C-9), 156.87 (C-2), 148.89 (C-4'), 145.21 (C-3'), 133.73 (c-3), 122.04 (C-6'), 121.60 (C-1'), 116.69 (C-5'), 115.67 (C-2'), 104.35 (C-10), 101.65 (C-1"), 101.20 (C-1'"), 99.36 (C-6), 94.06 (C-8), 76.89 (C-3"), 76.33 (C-5"), 72.29 (C-2"), 71.00 (C-4'"), 70.82 (C-3'"), 70.45(C-2'", C-5'"), 68.70 (C-4", C-6"), 18.20 (C-6'"). Compared with literature[28], it was identified as quercetin-3-O-rutinoside.

Methyl rosmarinate-huahewu4 (4): ^{1}H NMR (400 MHz, DMSO-d_6) δ: 1.83 (3H, s, H-2'"), 3.11 ~ 3.42 (6H, m, glc-1", 2", 3", 4", 5", 6"), 3.90 (3H, s, H-7-OMe), 4.95 (1H, d, J = 7.2 Hz, H-1"), 6.72 (1H, s, H-3), 6.85(1H, s, H-8), 6.88 (1H, d, J = 8.2 Hz, H-3'), 7.43 (2H, m, H-2",6'), 9.39 (1H, s, H-3'-OH), 10.00 (1H, s, H-4'-OH), 13.05 (1H, s, H-5-OH). ^{13}C NMR (100 MHz, DMSO- d_6) δ: 20.44 (C-2'"), 56.46 (C-OMe), 63.21 (C-6"), 70.03 (C-2"), 74.14 (C-2"), 76.55 (C-5"), 77.29 (C-3"), 91.52 (C-8), 102.09 (C-1"), 102.68 (C-3), 104.39 (C-10), 113.32 (C-2'), 115.85 (C-5'), 118.94 (C-6'), 121.28 (C-1'), 127.75 (C-6), 145.48 (C-3'), 149.74 (C-4'), 151.61 (C-9), 152.61 (C-5), 158.43 (C-7), 163.93 (C-2), 169.91 (C-1'"), 181.13 (C-4). Compared with literature[29], it was identified as Pedaliin-6"-acetate.

6,7,8,3',4'-Pentamethoxyflavone (5): ^{1}H NMR (400 MHz, DMSO-d_6) δ: 13.08 (OH-5), 10.36 (OH-4'), 7.98 (2H, d, J = 8.8 Hz, H-2', H-6'), 6.94 (1H, s, H-8), 6.93 (2H, d, J = 8.8 Hz, H-3', H-5'), 6.86 (1H, s, H-3), 5.14 (1H, m, OH-2"), 5.06 (1H, m, OH-3"), 5.04 (1H, m, OH-4"), 4.98 (1H, d, J = 5.2 Hz, OH-1"), 4.30 (1H, m, OH-5"), 4.13 (1H, dd, J = 5.0, 10.0 Hz, OH-6a"), 3.91 (3H, s, OCH_3-7), 3.59 (1H, dd, J = 4.5, 11.0 Hz, OH-6b"), ^{13}C NMR (100 MHz, DMSO-d_6) δ:182.71 (C-4), 164.48 (C-2), 161.76 (C-4'), 159.00 (C-7), 153.07 (C-9), 152.15 (C-5), 129.00 (C-2', C-6'), 128.58 (C-6), 121.58 (C-1), 116.43 (C-3', C-5'), 105.37 (C-10), 103.16 (C-1"), 102.46 (C-3), 92.12 (C-8), 77.76 (C-3"), 77.02 (C-5"), 74.61 (C-2"), 70.30 (C-4"), 61.34 (C-6"), 57.03 (OCH_3-7). Compared with literature[30], it was identified as 6,7,8,3',4'-Pentamethoxyflavone.

2.5 Prediction of α-glycosidase inhibitors

The a-glycosidase enzyme hydrolyzes polysaccharides and oligosaccharides into monosaccharides units, which play a key role in delivering the glucose into the blood[31]. Consequently, it is recommended that one of the best treatments is to delay the digestion of carbohydrates by inhibiting a-glycosidase enzyme, thereby reducing postprandial hyperglycemia to treat diabetes[32]. Molecular docking technology is applied to drug development, including the discovery of novel α-glycosidase inhibitors. Autodock is proved to be a powerful tool for evaluating the binding efficacy between ligands and protein targets[33]. The docking also predicts the binding orientation of the ligands to the active sites of α-glycosidase frequently[34]. Therefore, to find out anti-diabetic chemicals from *C. spicatus*, we have conducted virtual screening of 5 chemicals with the α-glycosidase enzyme by AutoDock. In the present study, molecular docking was applied to simulate the molecular recognition process between α-glycosidase and the compounds separated above from *C. spicatus* and the binding energies were calculated simultaneously. Amino acids contributed to substrate recognition by a combination force of electrostatic, hydrophobic, and hydrogen bonding interactions. The interaction details are listed in Table 2, including Affinity (kcal/mol), and the number of hydrogen bonds between the five compounds and α-glycosidase.

Table 2
The docking results of the five compounds to α-glycosidase

Compounds	Affinity kcal/mol	Number of H-bonds	Bonding residues	Bond length
2-Caffeoyl-L-tartaric acid	-7.7	3	ASP 1526	2.27
			ASP 1420	2.19
			ASP 1157	2.71
N-(E)-caffeoyldopamine	-8.3	0		
rosmarinc acid	-8.6	6	AGR 1510	2.77
			ASP 1526	1.86
			PHE 1560	2.25 (Aromatio H-bond)
			TRP 1355	2.48, 2.49 (Aromatio H-bond)
			TRP 1369	2.04
Methyl rosmarinate	-8.4	2	TRP 1355	2.41 (Aromatio H-bond)
			PHE 1560	2.14 (Aromatio H-bond)
6,7,8,3',4'-Pentamethoxyflavone	-7.6	0		

As a result, the five compounds can embed in the α-glycosidase cavity, and the compound 1, 3, and 4 were predominantly stable in the catalytic site by hydrogen bond and aromatio hydrogen bond (Fig. 7), and the affinity energies of the identified compounds ranged from − 7.6 to -8.6 kcal/mol, which are all

better than acarbose (-6.6 kcal/mol), indicating that the five compounds may have a potential to be a α-glycosidase inhibitor. In addition, according to Ruiz-Vargas et al., the α-glucosidase inhibitory activity of methyl rosmarinate shown 82.77 ± 2.10% of inhibition at 0.75 mM, and a Lineweaver-Burk double reciprocal plot confirmed that the higher α-glucosidase inhibitory activity of methyl rosmarinate is of non-competitive nature[35]. Alternatively, Giles-Rivas et al. confirmed that methyl rosmarinate (compound 4) exhibits significant anti-diabetic and anti-hyperglycemic activity, and its mechanism may be related to the overexpression of PPARγ, PPARα, GLUT-4 and FATP[36]. Among the five compounds, 6,7,8,3',4'-pentamethoxyflavone exhibited the highest affinity energy (-7.6 kcal/mol), while rosmarinc acid showed a lower affinity energy (-8.6 kcal/mol). Comparing the five compounds, the compound 3 showed the lowest affinity energy and have more H-bonds.

Compound 3 (rosmarinc acid) with the affinity energy of -8.6 kcal/mol occupied the active region by interfering with amino acid residues located in the binding cavity, such as AGR 1510, ASP 1526, PHE 1560, TRP 1355, and TRP 1369 (Fig. 8). In the conformation of α-glycosidase-compound 3 complex, there are three hydrogen bonds and three aromatio H-bonds. As shown in Fig. 8, two hydroxyl groups of the compound 3 formed the hydrogen bonds with the side-chain amino-group of AGR 1510and TRP 1369, and the length of hydrogen bonds were 2.77 Å and 2.04 Å respectively; a hydroxyl group of the compound 3 formed the hydrogen bond with the side-chain carboxyl group of ASP 1526, and the length of hydrogen bond was1.86 Å. Besides, the three aromatio H-bonds were formed by side-chainaromatic hydrogen of PHE 1560 and TRP 1355with the oxygen of the ligand molecule, and the length of hydrogen bonds were 2.25 Å, 2.49 Å and 2.48 Å respectively (Table 2). These hydrogen bonds overtly strengthened the interaction and anchored for binding the inhibitor in the active site. It is important to note that rosmarinc acid inhibited α-glucosidase activity in vitro (IC_{50}, 2.52 mM)[37]. Therefore, *C. spicatus* may be a good source for isolating rosmarinc acid, and for α-glucosidase inhibitory activity.

3. Conclusion

A simple, rapid and efficient method using HSCCC with continuous sample introduction was established for separation of five compounds with similar polarity from *C. spicatus*. Through HSCCC, the polarity similar compounds 2, 3 and 4 were separated in one step. In order to improve separation efficiency, the continuous sample introduction was used to reduce the time required for solvent equilibrium in the HSCCC process. Furthermore, the co-eluted components were purified by prep-HPLC. Then, predicting the active compounds by molecular docking. The result showed that the five compounds all have lower affinity energies than acarbose, and the compound 3 has the strongest hydrogen bond with α-glycosidase. The five compounds can be used for further study for their inhibition of α-glycosidase and further for dietetic approaches designed to manage T2D.

4. Materials And Methods

4.1 Plant materials

C. spicatus was purchased from the herb market of Bozhou, Anhui, China, in September 2019, and identified by Dr. X.P. Li. The dried whole plant (1.0 kg) of *C. spicatus* was crashed to coarse powder.

4.2 Reagents

Analytical grade reagents were used in extraction, MCI, HSCCC separation, which were purchased from the Jinan Reagent Factory (Jinan, China). Chromatographic grade reagents were used for HPLC analysis, which were purchased from Yuwang Chemical Ltd. (Shandong, China). Deionized water was used throughout the experiment.

4.3 Apparatus

The HSCCC used in the study is TBE-300B system with three polytetrafluoroethylene preparative coils (i.d. of the tubing = 1.6 mm, total volume = 280 mL) and a sample loop (20 mL) equipped with a model TBP5002 constant-flow pump (Tauto BiotechCo. Ltd., Shanghai, China), a model UV-500 detector (XUYUKJ Instruments, Hangzhou, China), and a model N2000 workstation (Zhejiang University, Hangzhou, China). ADC-0506 constant temperature-circulating implement (Shanghai Shunyu Hengping Instruments, Shanghai, China) was used to adjust the experiment temperature. The recycling HSCCC separation was carried out on TBE-300B system with a 6-port valve.

HPLC analysis was performed on an Agilent 1260 system (Agilent Technologies Co. Ltd., USA), which was equipped with a G1311C solvent delivery unit, a G1315D UV-DAD detector, a G1316A column thermostat, a G1329B auto sampler, and an Agilent HPLC workstation.

The nuclear magnetic resonance (NMR) spectrometer used in this study was a Mercury-400B NMR spectrometer (Varian Co. Ltd., USA).

4.4 Preparation of crude sample

The crude sample of *C. spicatus* powder (1.0 kg) was powdered and extracted with 70% ethanol (10 L × 3) ultrasonic extraction for 1 h. All filtrates were combined and concentrated to remove ethanol under reduced pressure by rotary evaporation at 60 ºC. The water solution was treated by vacuum freeze dryer at 5 ºC to obtain crude extract.

10 g of crude sample was dissolved in 50 mL of water, and then introduced into the MCI column. The column was then eluted by 20%, 40%, 60% and 80% methanol consecutively. The chromatogram was recorded at 254 nm. Each fraction from MCI was analyzed by HPLC. 40% methanol fraction from MCI column was chosen for further experiment (Figure. 1).

4.5 HSCCC process for separation of polarity similar compounds

4.5.1 Selection of two-phase solvent system

Choosing of solvent system used in HSCCC is based on the partition coefficient (*K*). The solvent system was selected by a 9 × 9 map-based solvent selection strategy[23], and the *K* of target compounds were determined by HPLC method.

4.5.2 Preparation of two-phasesolvent system and sample solution

Hexane/ethylacetate/methanol/water (HEMWat) (1.5% acetic acid) (3:5:3:5, v/v) was used in HSCCC process. Solvent system reached equilibrium at room temperature by fully shaken. The upper phase and the lower phase were then separated and degassed via ultrasonic bath for 30 min before use.

In HSCCC process, 20 mg of the sample was dissolved in 10 mL lower phase of the solvent system.

4.5.3 HSCCC separation procedure

HSCCC process was performed by the following steps. Firstly, the upper phase using as stationary phase was pumped into the multilayer column. Then, the apparatus was rotated at 800 rpm and the lower phase using as mobile phase was pumped into the column simultaneously. When hydrodynamic equilibrium was reached, sample solution was injected. During separation process, continuous injection system was used for enrichment of target compounds. The data was detected by a UV-500 detector and peak fractions were collected according to the HSCCC chromatogram.

4.6 HPLC analysis and identification of target compounds

HPLC analyses the 40% ethanol fraction of the MCI resin, fractions of HSCCC and prep-HPLC. Conditions: A Platisil ODS-C18 analytical column (4.6 × 250 mm, 5 μm) was used. Mobile phase was composed of 0.1% acid water (A) and methanol (B) with a gradient elution program: 0–30 min, 10–95% B; 30–40 min, 95% B. The flow rate was 1.0 mL/min, the column temperature was 30 °C and the detection wave length was 254 nm.

The chemical structures were elucidated by ^{1}H-NMR and ^{13}C-NMR.

4.7 Molecular docking

The energy of ligand molecules was minimized using Chem 3D 16.0. The X- ray crystal structure of α-glycosidase is download from RSCB database. Hydrogen atoms were added to the protein structure to ensure correct protonation states. Water molecules were not considered in the analyses. In all cases, the docking analysis was performed in a grid map of 18 × 20 × 20 with the spacing of 1 Å centered on the active site of α-glycosidase.

Declarations

Acknowledgements

This work was financially supported by the Joint Co-construction Project of Henan Medical Science and Technology Research Plan (LHGJ20190273).

Availability of data and materials

The datasets used or analyzed during the current study are available from the corresponding author on reasonable request.

Authors' contributions

Chunsheng Zhu and Hongjuan Niu contributed towards the concept and manuscript writing; Anzheng Nie and Meng Bian revised and supervised overall project. All authors read and approved the final version of manuscript.

Competing interests

The authors declare that they have no competing interest.

References

1. Ji, L. *et al.* Early combination versus initial metformin monotherapy in the management of newly diagnosed type 2 diabetes: An East Asian perspective. *Diabetes Obes Metab*, doi:10.1111/dom.14205 (2020).
2. Aynalem, S. B. & Zeleke, A. J. Prevalence of Diabetes Mellitus and Its Risk Factors among Individuals Aged 15 Years and Above in Mizan-Aman Town, Southwest Ethiopia, 2016: A Cross Sectional Study. *Int J Endocrinol* **2018**, 9317987, doi:10.1155/2018/9317987 (2018).
3. Scheen, A. J. Sodium-glucose cotransporter type 2 inhibitors for the treatment of type 2 diabetes mellitus. *Nat Rev Endocrinol* **16**, 556-577, doi:10.1038/s41574-020-0392-2 (2020).
4. Chase-Vilchez, A. Z., Chan, I. H. Y., Peters, S. A. E. & Woodward, M. Diabetes as a risk factor for incident peripheral arterial disease in women compared to men: a systematic review and meta-analysis. *Cardiovasc Diabetol* **19**, 151, doi:10.1186/s12933-020-01130-4 (2020).
5. Kerry, R. G. *et al.* Molecular prospect of type-2 diabetes: Nanotechnology based diagnostics and therapeutic intervention. *Rev Endocr Metab Disord*, doi:10.1007/s11154-020-09606-0 (2020).
6. Sharma, P., Joshi, T., Joshi, T., Chandra, S. & Tamta, S. Molecular dynamics simulation for screening phytochemicals as α-amylase inhibitors from medicinal plants. *J Biomol Struct Dyn*, 1-15, doi:10.1080/07391102.2020.1801507 (2020).
7. Song, Y., Xu, B. & Cai, W. Active substances and in vitro anti-diabetic effects of a traditional folk remedy Bian-Que Triple-Bean Soup as affected by the boiling time. *Food Funct* **4**, 635-643, doi:10.1039/c3fo30303a (2013).
8. Sepehri, N. *et al.* Synthesis, characterization, molecular docking, and biological activities of coumarin-1,2,3-triazole-acetamide hybrid derivatives. *Arch Pharm (Weinheim)* **353**, e2000109,

doi:10.1002/ardp.202000109 (2020).

9. Chiasson, J. L. *et al.* Acarbose treatment and the risk of cardiovascular disease and hypertension in patients with impaired glucose tolerance: the STOP-NIDDM trial. *Jama* **290**, 486-494, doi:10.1001/jama.290.4.486 (2003).
10. Kawamori, R. *et al.* Voglibose for prevention of type 2 diabetes mellitus: a randomised, double-blind trial in Japanese individuals with impaired glucose tolerance. *Lancet* **373**, 1607-1614, doi:10.1016/s0140-6736(09)60222-1 (2009).
11. Chen, W. D. *et al.* "Kidney Tea" and Its Bioactive Secondary Metabolites for Treatment of Gout. *J Agric Food Chem* **68**, 9131-9138, doi:10.1021/acs.jafc.0c03848 (2020).
12. Luo, Y. *et al.* Cytotoxic and renoprotective diterpenoids from Clerodendranthus spicatus. *Fitoterapia* **125**, 135-140, doi:10.1016/j.fitote.2018.01.003 (2018).
13. Li, Y. M., Xiang, B., Li, X. Z., Yan, Y. M. & Cheng, Y. X. New Diterpenoids from Clerodendranthus spicatus. *Nat Prod Bioprospect* **7**, 263-267, doi:10.1007/s13659-017-0128-8 (2017).
14. Luo, Y. *et al.* New ursane-type triterpenoids from Clerodendranthus spicatus. *Fitoterapia* **119**, 69-74, doi:10.1016/j.fitote.2017.04.001 (2017).
15. Ashraf, K., Sultan, S. & Adam, A. Orthosiphon stamineus Benth. is an Outstanding Food Medicine: Review of Phytochemical and Pharmacological Activities. *J Pharm Bioallied Sci* **10**, 109-118, doi:10.4103/jpbs.JPBS_253_17 (2018).
16. Azam, A. A. *et al.* Urinary metabolomics study on the protective role of Orthosiphon stamineus in Streptozotocin induced diabetes mellitus in rats via (1)H NMR spectroscopy. *BMC Complement Altern Med* **17**, 278, doi:10.1186/s12906-017-1777-1 (2017).
17. Wang, X. *et al.* A rapid and practical prediction method for the Arizona solvent system family used in high speed countercurrent chromatography. *J Chromatogr A* **1629**, 461426, doi:10.1016/j.chroma.2020.461426 (2020).
18. Tong, S., Guan, Y. X., Yan, J., Zheng, B. & Zhao, L. Enantiomeric separation of (R, S)-naproxen by recycling high speed counter-current chromatography with hydroxypropyl-β-cyclodextrin as chiral selector. *J Chromatogr A* **1218**, 5434-5440, doi:10.1016/j.chroma.2011.06.015 (2011).
19. Liu, Q. *et al.* Separation of polyphenols from leaves of Malus hupehensis (Pamp.) Rehder by off-line two-dimensional High Speed Counter-Current Chromatography combined with recycling elution mode. *Food Chem* **186**, 139-145, doi:10.1016/j.foodchem.2014.09.037 (2015).
20. Sutherland, I. A. & Fisher, D. Role of counter-current chromatography in the modernisation of Chinese herbal medicines. *J Chromatogr A* **1216**, 740-753, doi:10.1016/j.chroma.2008.11.095 (2009).
21. Hopkins, A. L. Network pharmacology: the next paradigm in drug discovery. *Nat Chem Biol* **4**, 682-690, doi:10.1038/nchembio.118 (2008).
22. Walker, S. & McEldowney, S. Molecular docking: a potential tool to aid ecotoxicity testing in environmental risk assessment of pharmaceuticals. *Chemosphere* **93**, 2568-2577, doi:10.1016/j.chemosphere.2013.09.074 (2013).

23. Ito, Y. Golden rules and pitfalls in selecting optimum conditions for high-speed counter-current chromatography. *J Chromatogr A* **1065**, 145-168, doi:10.1016/j.chroma.2004.12.044 (2005).
24. Liang, J., Meng, J., Wu, D., Guo, M. & Wu, S. A novel 9 × 9 map-based solvent selection strategy for targeted counter-current chromatography isolation of natural products. *J Chromatogr A* **1400**, 27-39, doi:10.1016/j.chroma.2015.04.043 (2015).
25. Wang, W. *et al.* A novel chromatographic separation method for rapid enrichment and isolation of novel flavonoid glycosides from Sphaerophysa salsula. *J Sep Sci* **43**, 4018-4027, doi:10.1002/jssc.202000688 (2020).
26. X. Tao, N. Xu, X. Wang, N. Guo, & Q. Chen. Organic acids derived from Picris davurica and their anti-oxidative activity. *Chinese Traditional and Herbal Drugs* **47,**544-548, doi: 10.7501/j.issn.0253-2670.2016.04.003 (2016).
27. Kokubun, T., Kite, G. C., Veitch, N. C. & Simmonds, M. S. Amides and an alkaloid from Portulaca oleracea. *Nat Prod Commun* **7**, 1047-1050 (2012).
28. Q. Shi, J. Zhao, J. Dang, X. Yuan, & Q. Wang. Triterpenes, Flavonoids, and Lignans from Dracocephalum heterophyllum. *Chem Nat Compd* **54**, 970-972, doi: 10.1007/s10600-018-2524-7 (2018).
29. Al-Musayeib, N., Perveen, S., Fatima, I., Nasir, M. & Hussain, A. Antioxidant, anti-glycation and anti-inflammatory activities of phenolic constituents from Cordia sinensis. *Molecules* **16**, 10214-10226, doi:10.3390/molecules161210214 (2011).
30. Han, S., Kim, H. M., Lee, J. M., Mok, S. Y. & Lee, S. Isolation and identification of polymethoxyflavones from the hybrid Citrus, hallabong. *J Agric Food Chem* **58**, 9488-9491, doi:10.1021/jf102730b (2010).
31. Taslimi, P. & Gulçin, İ. Antidiabetic potential: in vitro inhibition effects of some natural phenolic compounds on α-glycosidase and α-amylase enzymes. *J Biochem Mol Toxicol* **31**, doi:10.1002/jbt.21956 (2017).
32. Lolak, N. *et al.* Synthesis, characterization, inhibition effects, and molecular docking studies as acetylcholinesterase, α-glycosidase, and carbonic anhydrase inhibitors of novel benzenesulfonamides incorporating 1,3,5-triazine structural motifs. *Bioorg Chem* **100**, 103897, doi:10.1016/j.bioorg.2020.103897 (2020).
33. Adinarayana, K. P. & Devi, R. K. Protein-Ligand interaction studies on 2, 4, 6- trisubstituted triazine derivatives as anti-malarial DHFR agents using AutoDock. *Bioinformation* **6**, 74-77, doi:10.6026/97320630006074 (2011).
34. Kharkar, P. S., Warrier, S. & Gaud, R. S. Reverse docking: a powerful tool for drug repositioning and drug rescue. *Future Med Chem* **6**, 333-342, doi:10.4155/fmc.13.207 (2014).
35. Ruiz-Vargas, J. A. *et al.* α-Glucosidase inhibitory activity and in vivo antihyperglycemic effect of secondary metabolites from the leaf infusion of Ocimum campechianum mill. *J Ethnopharmacol* **243**, 112081, doi:10.1016/j.jep.2019.112081 (2019).
36. Giles-Rivas, D. *et al.* Antidiabetic effect of Cordia morelosana, chemical and pharmacological studies. *J Ethnopharmacol* **251**, 112543, doi:10.1016/j.jep.2020.112543 (2020).

37. Zhu, F. *et al.* Rosmarinic acid and its ester derivatives for enhancing antibacterial, α-glucosidase inhibitory, and lipid accumulation suppression activities. *J Food Biochem* **43**, e12719, doi:10.1111/jfbc.12719 (2019).

Figures

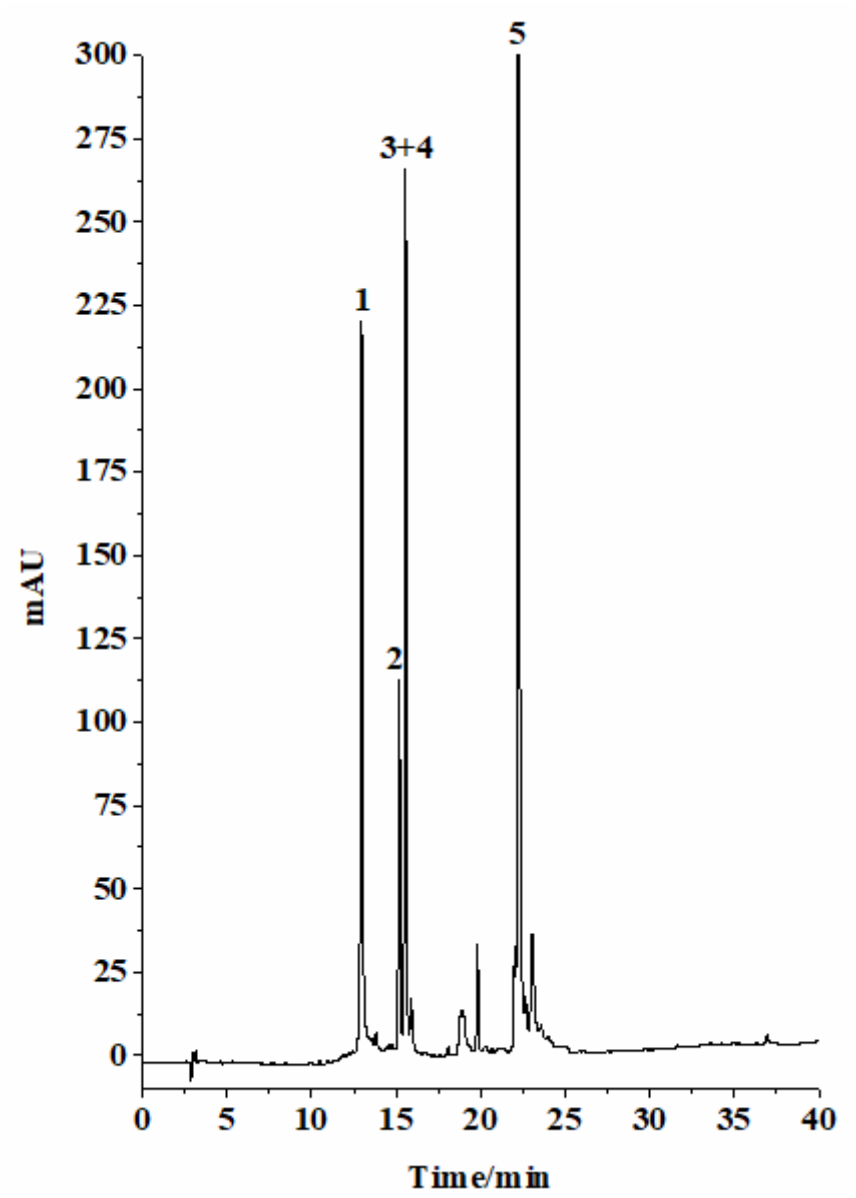

Figure 1

HPLC chromatogram of 40% methanol fraction from MCI column. Conditions: column, Platisil ODS-C18 analytical column (250 mm × 4.6 mm i.d., 5μm); mobile phase, 0.1% acid water (A) and methanol (B), gradient elution program: 0-30 min, 10-95% B; 30-40 min, 95% B; flow rate, 1.0 mL/min; temperature, 30°C; detection wavelength, 254 nm.

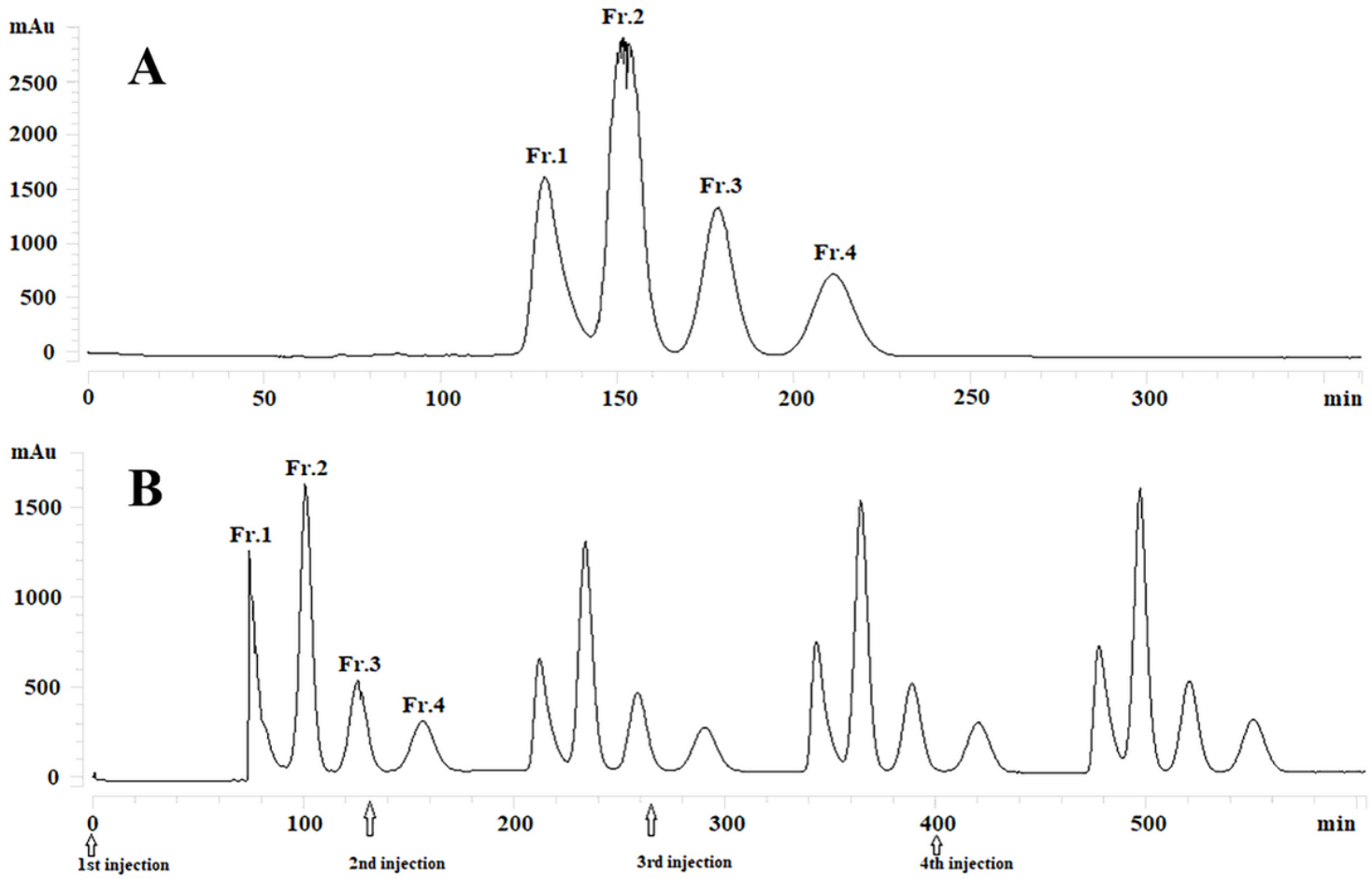

Figure 2

HSCCC chromatogram of 40% methanol fraction using n-hexane-ethyl acetate-methanol-water (3:5:3:5, v/v) (1.5 % acetic acid). Conditions: stationary phase, upper phase; revolution speed, 800 rpm; separation temperature, 30 °C; detection wavelength, 320 nm; flow rate, 2.0 ml/min (A: Single injection; B: forth continuous sample injection).

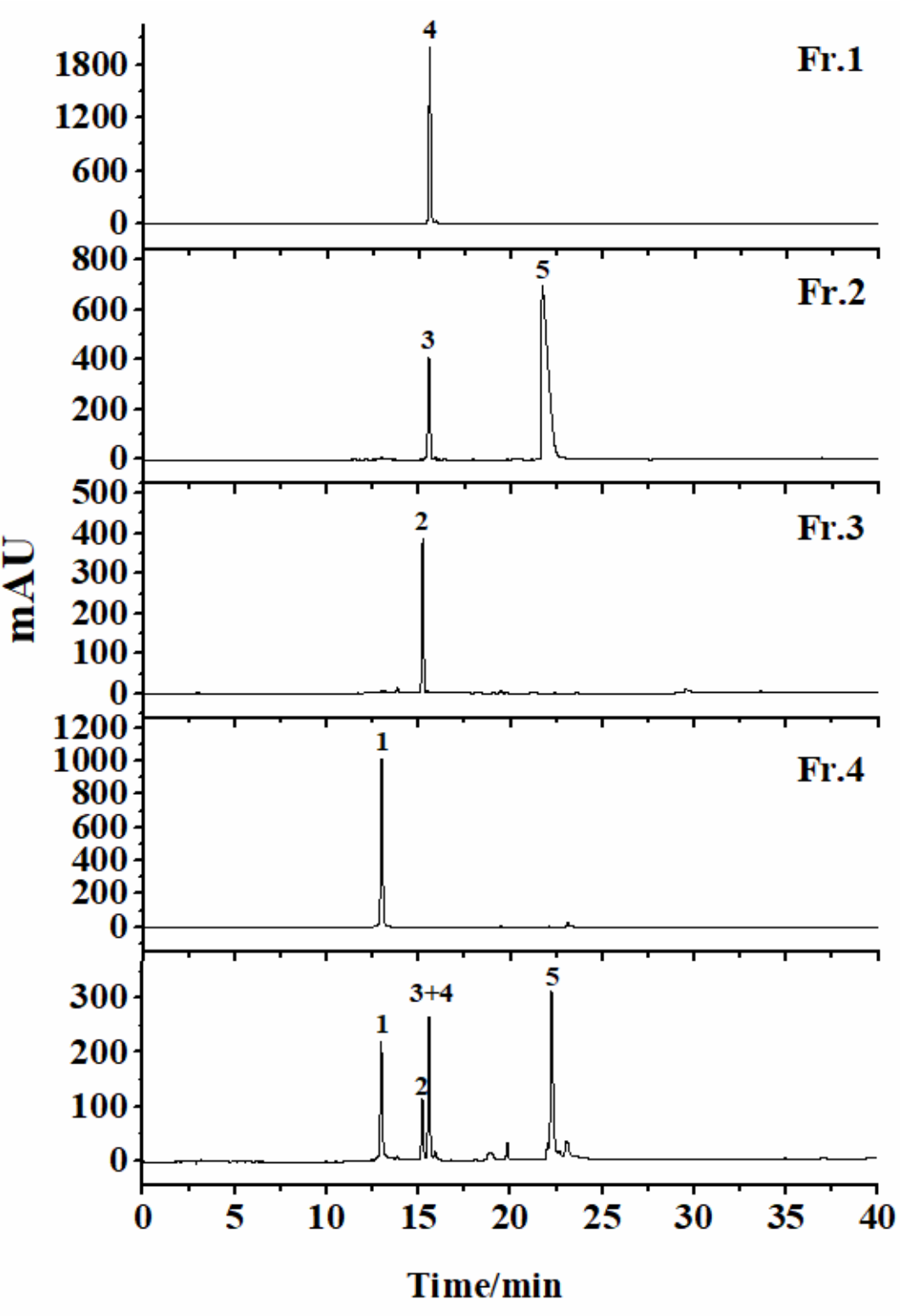

Figure 3

HPLC analysis of four fractions from HSCCC. Conditions: column, Platisil ODS-C18 analytical column (250 mm × 4.6 mm i.d., 5μm); mobile phase, 0.1% acid water (A) and methanol (B), gradient elution program: 0-30 min, 10-95% B; 30-40 min, 95% B; flow rate, 1.0 mL/min; temperature, 30°C; detection wavelength, 254 nm.

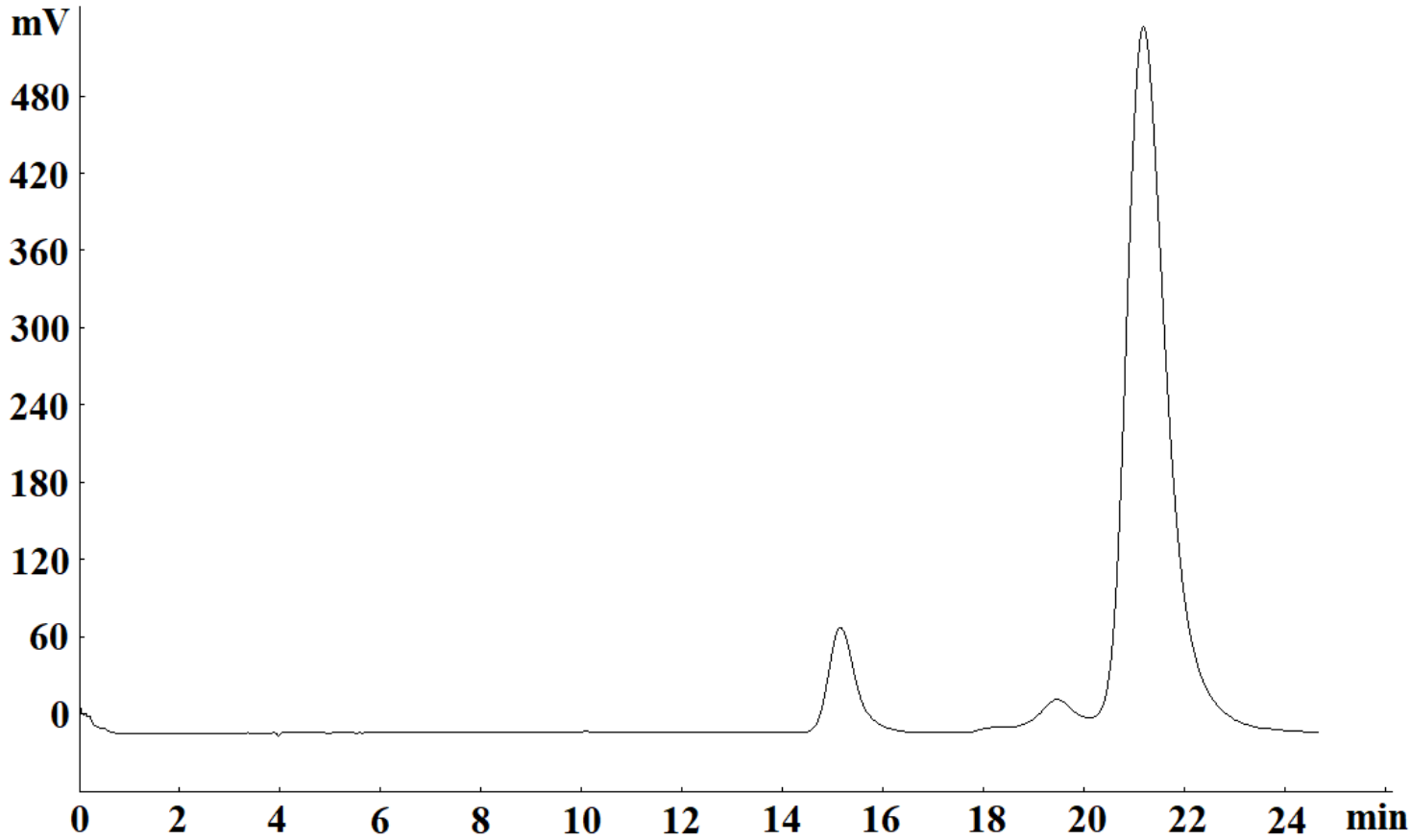

Figure 4

Prep-HPLC chromatogram of fraction 2 from HSCCC. Conditions: column, Reprosil 100 C18 column (250×20 mm i.d., 10 μm); mobile phase, 40% methanol; flow rate, 18 mL/min; detection wavelength, 254 nm.

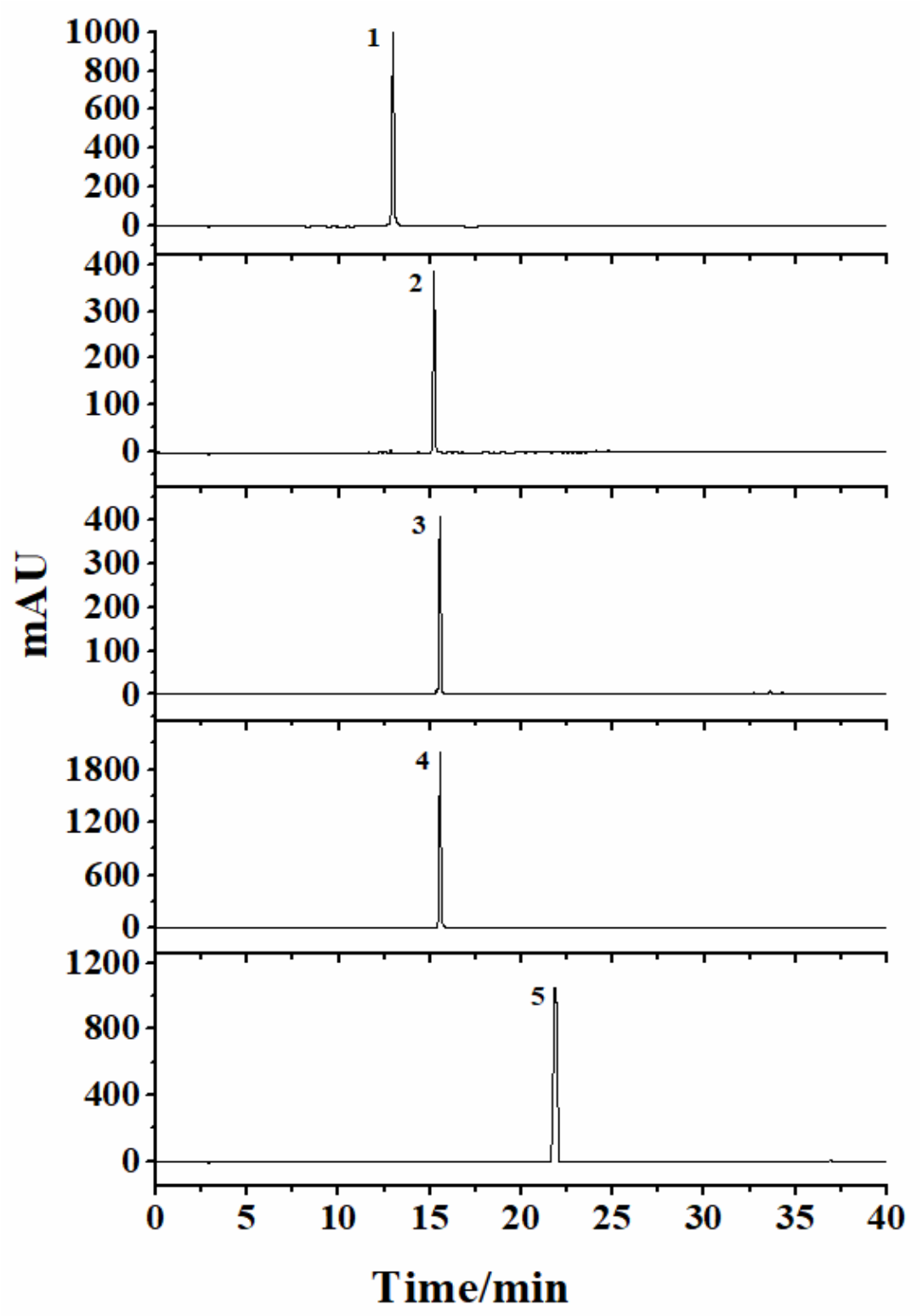

Figure 5

Purity detection of the five compounds by HPLC. Conditions: column, Platisil ODS-C18 analytical column (250 mm × 4.6 mm i.d., 5μm); mobile phase, 0.1% acid water (A) and methanol (B), gradient elution program: 0-30 min, 10-95% B; 30-40 min, 95% B; flow rate, 1.0 mL/min; temperature, 30°C; detection wavelength, 254 nm.

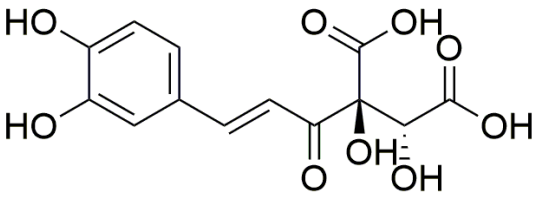

1. 2-caffeoyl-L-tartaric acid

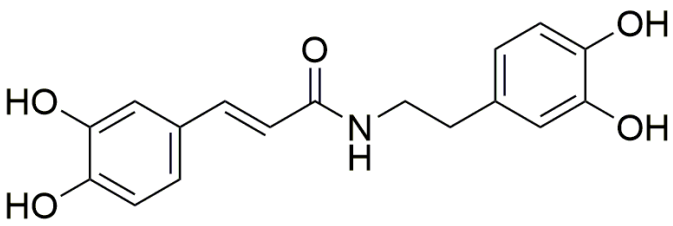

2. N-(E)-caffeoyldopamine

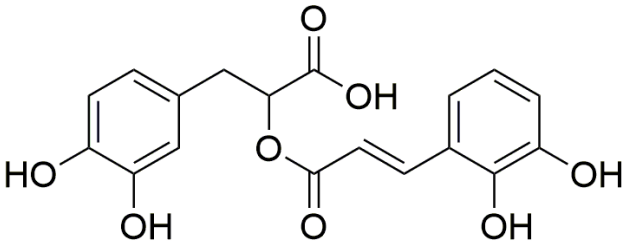

3. rosmarinc acid

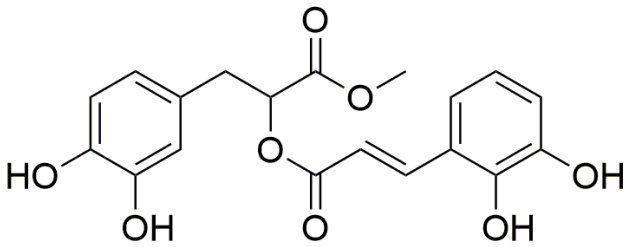

4. methyl rosmarinate

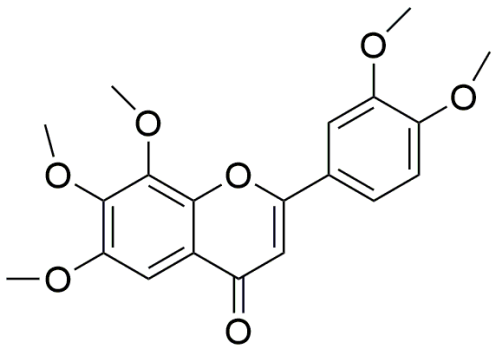

5. pentamethoxyflavone

Figure 6

The chemical structures of the five compounds.

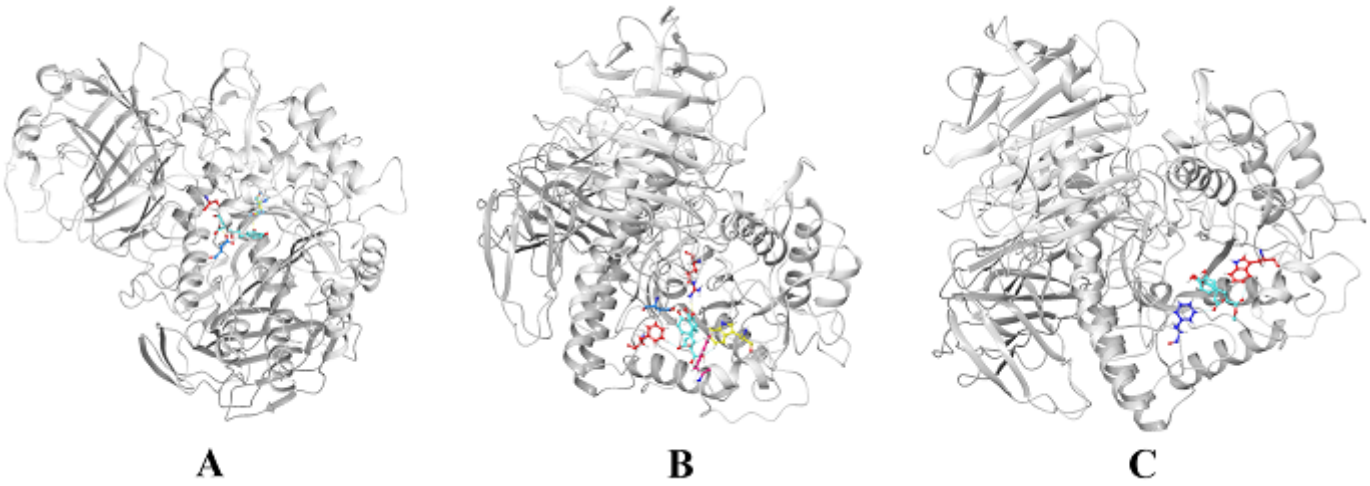

Figure 7

Molecular docking models of α-glycosidase and compounds 1 (A), 3 (B), and 4 (C).

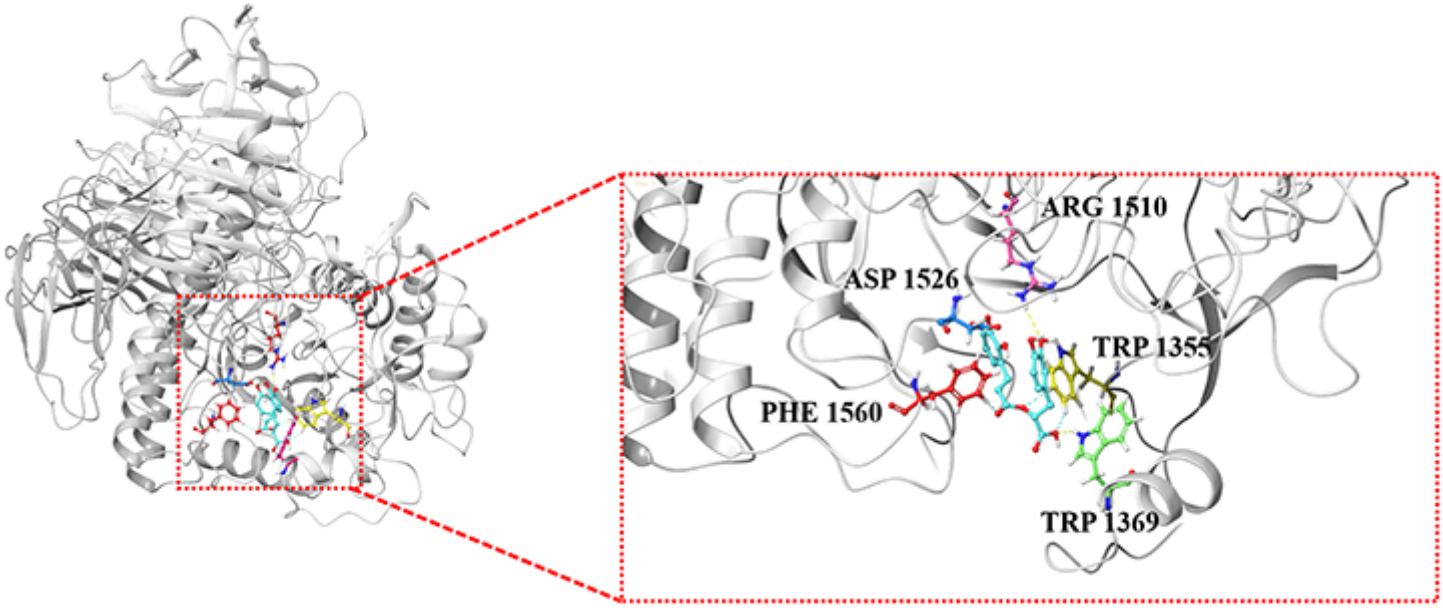

Figure 8

Molecular docking models of α-glycosidase and compound 3 with overall view and enlarged view.